





Article

Reduction of Induction Motor Energy Consumption via Variable Velocity and Flux References

Jorge Resa ^{1,*}, Domingo Cortes ^{1,†}, Juan Francisco Marquez-Rubio ^{1,†}
and David Navarro ^{2,‡}

¹ Instituto Politecnico Nacional, ESIME Culhuacan, Mexico City 04440, Mexico

² Escuela de Ingeniería y ciencias, Tecnológico de Monterrey, CCM, Mexico City 14380, Mexico

* Correspondence: jrtpn@gmail.com; Tel.: +52-55-5435-0059

† Avenida Santa Ana 951, Coyoacan 04440, CDMX, Mexico.

‡ Calle del Puente 222, Tlalpan 14380, CDMX, Mexico.

Received: 31 May 2019; Accepted: 26 June 2019; Published: 29 June 2019



Abstract: Induction motors (IM) have been a fundamental part of industrial applications for over a century and the number of their applications continues to expand. A significant amount of the world's total energy expense is consumed by this kind of motor. Hence, it is very important to increase the energy efficiency of these machines. Due to its good performance, field-oriented control (FOC) is the most common strategy to control IM. FOC requires references for stator current and rotor magnetic fluxes. For velocity regulation, a velocity reference is used instead of a stator current reference. However, at motor start-up or when a change of torque is required, it would be convenient for these references to be variable in order to reduce energy consumption. In this work, it is shown that this is indeed the case, and a technique to find optimal time-variable references for stator currents and magnetic rotor fluxes to reduce energy consumption is proposed. It is shown that, depending on the mechanical load, an energy reduction of 20–45% can be achieved.

Keywords: energy efficiency; induction motor control; field-oriented control; optimization applications

1. Introduction

The reduction of energy consumption is a very important issue nowadays. Great effort is being dedicated to reducing the energy used by electric and electronic devices, particularly in two general cases: (a) in commonly used devices and (b) in devices fed by batteries. The first case is important because any improvement in energy expenditure in these devices has a multiplicative effect. The importance of the second case is obvious, as it is always desirable to maximize battery charge duration.

Induction motors are ubiquitous in industry, to the extent that more than 30% of the world's total energy consumption comes from this kind of motor [1,2]. In addition, their use in electric transportation is increasing. Hence, any improvement in the energy expenditure of these machines is important.

Energy consumption optimization in three-phase induction motors has been a widely discussed topic since the first electronic converters were used to drive this type of motor [3,4]. With the introduction of the Field-Oriented Control (FOC), attention on this topic became deeper. This control strategy seeks to directly modifying the dynamics of the current that drives the motor. The FOC acts over the motor flux (d -axis) and current vector (q -axis). The significance of these vectors is due to the resultant torque from their product, and the energy consumption is proportional to their magnitude. Hence, it is natural that many works on optimization have relied on the FOC as a base [5].

Many previously published works have focused on obtaining optimal values for gains of controllers of the FOC. Some works have shown that a change in the gain modifies the resulting performance of the motor [6–8]. Other works have focused on the selection of an appropriate set-point

for the optimal magnetic flux, given a certain load. Once the set-point is found, it is kept constant, even if the motor starts or stops numerous times [9–11]. In [12], the approach of minimizing the power losses in the stator to find the correct references for the controllers was employed. To find the set-point value, some studies have used numerical methods [13]. Others found the value using more heuristic techniques such as genetic algorithms or swarm algorithms [14].

A significant amount of energy is consumed by the motor when torque or velocity changes, particularly at the start-up of the motor or when an increase in torque is required. In this dynamic situation, to reduce energy consumption, it would be convenient for fluxes and current to be variable. However, most works keep the fluxes constant. Taking this observation into account, in this paper, a procedure to find references for flux and current vectors that minimize the motor energy consumption is proposed. The proposed algorithm seeks two time-variable functions that act as references for the flux and current vectors.

The proposed optimization procedure uses the whole dynamic system equations, including the motor dynamical model, a static or dynamical model for the mechanical load, and dynamic controller equations. The cost function to be minimized is constructed from the supplied currents, which are directly related to the total energy consumption.

It is important to point out that, for the optimization procedure, it is a controller strategy is assumed to be given. Thus, the controller parameters and final values of the set points are assumed to be known. There are some proposals to find optimal values for these parameters [15]. The procedure proposed here does not substitute, but rather complements, these proposals.

A control strategy that has proven to be very robust in simulations and in experiments [16] is employed in this paper. This control strategy includes proportional-integral (PI) controllers for the flux vector and the current vector. It also includes a third PI controller for the speed. Note that, although a control strategy is necessary to obtain the results, a different control strategy could be used in the optimization procedure.

As a result of the optimization procedure, time-variable vectors of flux and current are obtained as references. Using such references, the actual variables have peak values that are notably lower than those achieved without optimization. More significantly, average power at motor start-up is 20–45% lower.

The proposed procedure to find variable references requires a great number of calculations which must be performed before the motor operations. However, there are many applications where velocity changes are previously known. These applications include battery-fed motors, high peak starting current motors, and motors that continuously start and stop.

The rest of the paper is organized as follows: in Section 2, the overall setting for control of the induction motor is described. In Section 3, the optimization procedure is explained. Simulation results are presented in Section 4. The performance of the system before and after optimization is also analyzed in Section 4. In the last section, the benefits and limitations of the proposed procedure are discussed.

2. System Model

To obtain optimized references, it is necessary to build a complete model of the system. Such model can be derived by dividing the system into three parts: the induction motor model, the controller model including the magnetic flux estimator model, and the mechanical load model. In this work, a constant mechanical load is considered, but it would not be difficult to include a dynamic model for the load. In the following subsections, the motor model and the controller model are established.

2.1. The Model of the Induction Motor

The induction motor is an electro-mechanical device that has been studied extensively [4,5,17,18]. Basically, it consists of three stator coils, respectively fed by three (usually) sinusoidal voltages with 120° of phase between them. The current through the coils generated by the stator voltages results

in a rotating electromagnetic field. This electromagnetic field induces currents in the rotor formed by short-circuited bars. Currents through bars on the rotor cause a second field to be generated. The interaction between the stator field and rotor field produces torque.

The mathematical model of the induction motor can be derived from relations between stator current equations, the magnetic rotor flux equations, and a final equation that relates the electric torque to the mechanical torque [17–19]. Some works have developed models from relations between the three phase stator voltages $V_{a,b,c}$, stator currents $i_{a,b,c}$, and magnetic fluxes $\psi_{a,b,c}$.

It is well known that stator voltages and currents are not independent, and transformations can be made to describe a system using two instead of three phases. This is known as the Clarke transformation [20]. The two voltages (and currents) obtained after the Clarke transformation are separated by 90° and are known as the dq -frame.

Considering all the previous observations given in [17], the following model was obtained:

$$i_{ds}^s = -\frac{(L_m^2 R_r + L_r^2 R_s)}{\sigma L_r^2 L_s} i_{ds}^s + \frac{L_m R_r}{\sigma L_r^2 L_s} \psi_{dr}^s + \frac{L_m \omega_r}{\sigma L_r L_s} \psi_{qr}^s + \frac{V_{dr}^s}{\sigma L_s}, \tag{1a}$$

$$i_{qs}^s = -\frac{(L_m^2 R_r + L_r^2 R_s)}{\sigma L_r^2 L_s} i_{qs}^s + \frac{L_m R_r}{\sigma L_r^2 L_s} \psi_{qr}^s - \frac{L_m \omega_r}{\sigma L_r L_s} \psi_{dr}^s + \frac{V_{qr}^s}{\sigma L_s}, \tag{1b}$$

$$\psi_{dr}^s = \frac{L_m R_r}{L_r} i_{ds}^s - \frac{R_r}{L_r} \psi_{dr}^s - \psi_{qr}^s \omega_r, \tag{1c}$$

$$\psi_{qr}^s = \frac{L_m R_r}{L_r} i_{qs}^s - \frac{R_r}{L_r} \psi_{qr}^s + \psi_{dr}^s \omega_r, \tag{1d}$$

$$\dot{\omega}_r = P \left(\frac{3PL_m(i_{qs}^s \psi_{dr}^s - i_{ds}^s \psi_{qr}^s)}{(2J)4L_r} - \frac{T_L}{2J} \right). \tag{1e}$$

The symbols of model (1) are physical motor parameters and variables. They are defined in Table 1, except for σ , L_s , and L_r , which are introduced to simplify the notation and are given by

$$\sigma = 1 - \frac{L_m^2}{L_s L_r}, \tag{2a}$$

$$L_s = L_{ls} + L_m, \tag{2b}$$

$$L_r = L_{lr} + L_m. \tag{2c}$$

Table 1. Induction motor parameters.

Parameter	Description
i_{ds}^s	Supply current d -axis
i_{qs}^s	Supply current q -axis
ψ_{dr}^s	Rotor magnetic flux d -axis
ψ_{qr}^s	Rotor magnetic flux q -axis
V_{dr}^s	Supply voltage d -axis
V_{qr}^s	Supply voltage q -axis
ω_r	Motor angular velocity
T_L	Mechanic load torque
R_r	Rotor resistance
R_s	Stator resistance
L_{ls}	Stator inductance
L_{lr}	Rotor inductance
L_m	Mutual inductance
J	Rotor inertia
P	Number of poles

2.2. Field-Oriented Control of the Induction Motor

The voltages, currents, and magnetic fluxes of induction motors are time-variable. However, if a rotating coordinated frame synchronized with the rotor magnetic flux is defined, for these coordinates, electric and magnetic variables would be constants. Having electric and magnetic variables as constants, the magnitude of these variables could be controlled with the usual PI controllers to achieve maximum torque. These are the key ideas of FOC. The overall scheme of FOC is depicted in Figure 1. In what follows, the main components of this schema are described.

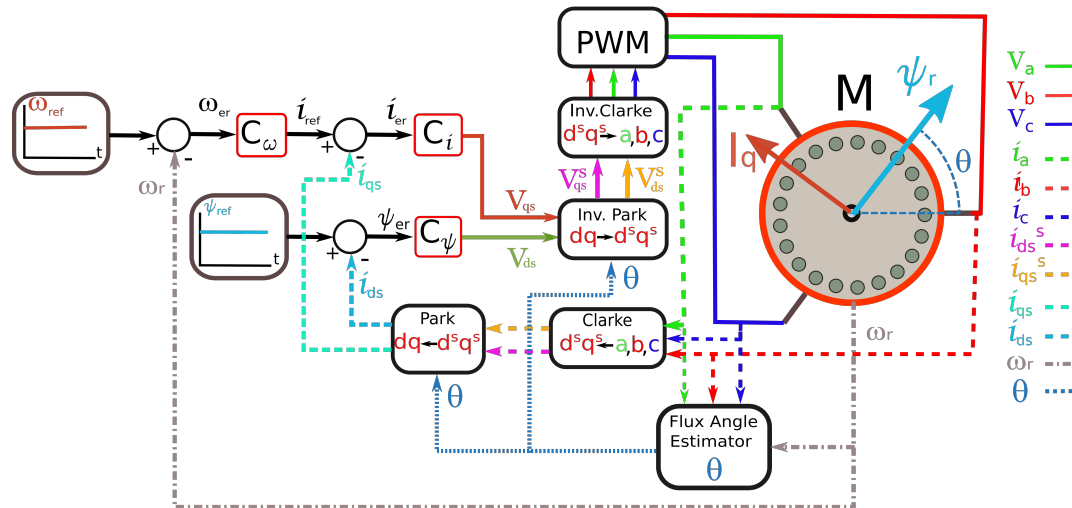


Figure 1. Velocity Field-Oriented Control.

2.2.1. Estimation of the Magnetic Flux Angle

To construct the rotating coordinate frame, it is necessary to know the direction of the magnetic flux of the rotor. The angle between the magnetic flux and the motor stator describes this direction. This angle is denoted by θ (see Figure 1). However, this angle can not be measured; hence, it must be estimated.

Several flux angle estimators have been proposed. The Voltage Model uses supplied voltages and stator currents. The Current Model uses stator currents and the rotor angular velocity. There are also several sensor-less techniques that do not need the angular velocity of the rotor, such as observers or slip estimators. Each estimation method has its advantages and disadvantages. Sensor-less methods do not need the velocity or position sensor, but they require a higher number of calculations.

The estimation model used in this work is known as the Voltage Model [17]. In the voltage model, the stator magnetic flux dq components are obtained from

$$\dot{\hat{\psi}}_{ds}^s = V_{ds}^s - R_s i_{ds}^s, \tag{3a}$$

$$\dot{\hat{\psi}}_{qs}^s = V_{qs}^s - R_s i_{qs}^s. \tag{3b}$$

Then, the rotor magnetic flux dq components are calculated using

$$\hat{\psi}_{dr}^s = \frac{L_r (\hat{\psi}_{ds}^s - L_{ls} i_{ds}^s)}{L_m} - L_{lr} i_{ds}^s, \tag{4a}$$

$$\hat{\psi}_{qr}^s = \frac{L_r (\hat{\psi}_{qs}^s - L_{ls} i_{qs}^s)}{L_m} - L_{lr} i_{qs}^s. \tag{4b}$$

Having the dq components of rotor flux estimation, the magnitude of the rotor flux is calculated using

$$\hat{\psi}_r^s = \sqrt{\hat{\psi}_{dr}^{s2} + \hat{\psi}_{qr}^{s2}}. \tag{5}$$

Finally, $\sin(\theta)$ and $\cos(\theta)$ are obtained from rotor magnetic flux estimation components and its magnitude:

$$\cos(\theta) = \frac{\hat{\psi}_{dr}^s}{\hat{\psi}_r^s}, \quad (6a)$$

$$\sin(\theta) = \frac{\hat{\psi}_{qr}^s}{\hat{\psi}_r^s}. \quad (6b)$$

Expressions (6) are used to construct the rotating coordinate transformation and its inverse.

2.2.2. The Park Transformation

In order to use Proportional-Integral controllers, a rotating frame needs to be used. In this rotating frame, all of the electric and magnetic variables can be seen as stationary vectors. This frame can be aligned to any vector in particular. Generally, this rotation frame is aligned with a magnetic flux vector, which can be the rotor flux or the stator flux.

In summary, the motor model has a stationary coordinate frame (denoted with super index s), and the controller has a rotating coordinate frame. In order to be used in the controller, the variables from the motor model have to be transformed with the Park transformation given by

$$\begin{bmatrix} i_{qs} \\ i_{ds} \end{bmatrix} = \begin{bmatrix} \cos(\theta) & -\sin(\theta) \\ \sin(\theta) & \cos(\theta) \end{bmatrix} \begin{bmatrix} i_{qs}^s \\ i_{ds}^s \end{bmatrix}. \quad (7)$$

2.2.3. The PI Controllers

To control the motor velocity via FOC, it is necessary to have three control loops. One control loop acts over the magnetic flux, a second control loop acts over the rotor current, and the third is a velocity control loop. The output of the velocity control loop can act as a reference for the rotor current control loop.

The control structure C_ψ (see Figure 1) acts over the rotor flux, and it is described by

$$\psi_{er} = \psi_{ref} - i_{ds}, \quad (8a)$$

$$\dot{\psi}_{ie} = \psi_{er}, \quad (8b)$$

$$V_{ds} = k_{a\psi}\psi_{er} + k_{b\psi}\dot{\psi}_{ie}, \quad (8c)$$

where ψ_{ref} is the reference of the magnetic flux.

Controller C_ω acts over the angular velocity while controller structure C_i acts over the rotor current, which produces torque. The output signal of C_ω is the reference for C_i .

The structure of controller C_ω is given by

$$\omega_{er} = \omega_{ref} - \omega_r, \quad (9a)$$

$$\dot{\omega}_{ie} = \omega_{er}, \quad (9b)$$

$$i_{sp} = k_{a\omega}\omega_{er} + k_{b\omega}\dot{\omega}_{ie}, \quad (9c)$$

where ω_{ref} is the reference for the rotor angular velocity.

Controller C_i uses i_{ref} as the reference, hence

$$i_{er} = i_{ref} - i_{qs}, \quad (10a)$$

$$\dot{i}_{ie} = i_{er}, \quad (10b)$$

$$V_{qs} = k_{ai}i_{er} + k_{bi}\dot{i}_{ie}. \quad (10c)$$

Finally, controller output voltages V_{ds} and V_{qs} must be converted from the rotating frame to the fixed frame using the inverse of the Park transformation given by

$$\begin{bmatrix} V_{qs}^s \\ V_{ds}^s \end{bmatrix} = \begin{bmatrix} \cos(\theta) & \sin(\theta) \\ -\sin(\theta) & \cos(\theta) \end{bmatrix} \begin{bmatrix} V_{qs} \\ V_{ds} \end{bmatrix}. \tag{11}$$

The gains of the three PI controllers depend on motor parameters such as the inductance and resistance as well as other performance parameters such as the damping factor and bandwidth.

The gains for controller C_i are given by

$$k_{ai} = L_{sr}, \tag{12a}$$

$$k_{bi} = \frac{R_r + R_s}{L_{sr}}, \tag{12b}$$

where

$$L_{sr} = (L_{ls} + L_m) \left(1 - \frac{L_m^2}{(L_{lr} + L_m)(L_{ls} + L_m)} \right). \tag{13}$$

The gains for controller for controller C_ψ are

$$k_{a\psi} = L_{sr}, \tag{14a}$$

$$k_{b\psi} = \frac{R_s}{L_{sr}}, \tag{14b}$$

where

$$k_{pr} = \frac{3P i_{\psi c} L_m^2}{4(L_{lr} + L_m)}. \tag{15}$$

Finally, the gains for controller C_ω are given by

$$k_{a\omega} = \frac{1}{k_t k_{pr}}, \tag{16a}$$

$$k_{b\omega} = \frac{1}{\delta^2}, \tag{16b}$$

where the parameters δ and k_t are proposed by the user based on the damping ratio and velocity sensor time constant.

3. The Proposed Procedure to Find Variable References

This section describes how the references for velocity ω_{ref} and flux ψ_{ref} are found. A variational approach is used. Optimization based on variational tools has been studied in many references (see, for example, the excellent books [21–23])

The main result of variational approach used in this work is summarized below, and then the specific procedure is detailed.

3.1. A Variational Tool

Consider the system

$$\dot{x} = f(x, u), \tag{17}$$

where $x \in \mathbb{R}^n, u \in \mathbb{R}^m, y, f: \mathbb{R}^{n+m} \rightarrow \mathbb{R}^n$. To find an input u^* that causes the system (17) to follow a trajectory x^* that minimizes the functional

$$J(u) = h(x(t_f)) + \int_{t_0}^{t_f} F(x, u) dt, \tag{18}$$

it is necessary that, for all $t \in [t_0, t_f]$, expressions

$$\dot{x}^* = \frac{\partial}{\partial p} \mathcal{H}(x^*, u^*, p^*), \tag{19a}$$

$$\dot{p}^* = -\frac{\partial}{\partial x} \mathcal{H}(x^*, u^*, p^*), \tag{19b}$$

$$0 = -\frac{\partial}{\partial u} \mathcal{H}(x^*, u^*, p^*), \tag{19c}$$

and boundary conditions

$$\left[\frac{\partial}{\partial x} h(x^*(t_f), t_f) - p^*(t_f) \right]^T \delta x_f = 0 \tag{20}$$

hold. Function $p(t)$ is a vector function in \mathbb{R}^n . The function \mathcal{H} is called the Hamiltonian and is defined by

$$\mathcal{H}(x, u, p) = F(x, u) + p^T f(x, u). \tag{21}$$

There are several methods to find u^* , x^* and p^* that satisfy optimal conditions (19). The steepest descent is an iterative method that is easy to understand. The method is summarized in Figure 2. First, an initial discretized $u(t)$ for $t \in [t_0, t_f]$ is proposed. Using u , the estate x^* is found by forward simulation, and the co-estate is found by backward simulation. At each iteration, small improvements are made by changing u according to

$$u^{(k+1)} = u^{(k)} - \tau \frac{\partial}{\partial u} \mathcal{H}^{(k)}, \tag{22}$$

where τ is the step size and can be constant or variable. If τ is constant, it must be smaller than the smallest valley. Changes in u given by Equation (22) seek to achieve

$$\left\| \frac{\partial}{\partial u} \mathcal{H}(x, u, p) \right\| = 0. \tag{23}$$

Note that, at each iteration, conditions (19a) and (19b) are satisfied. Then, if condition (19c) is fulfilled, it means that all optimal conditions (19) are accomplished. That is, when Equation (23) is accomplished, conditions (19) are fulfilled.

The algorithm stops when the left-hand-side of Equation (23) is close enough to zero.

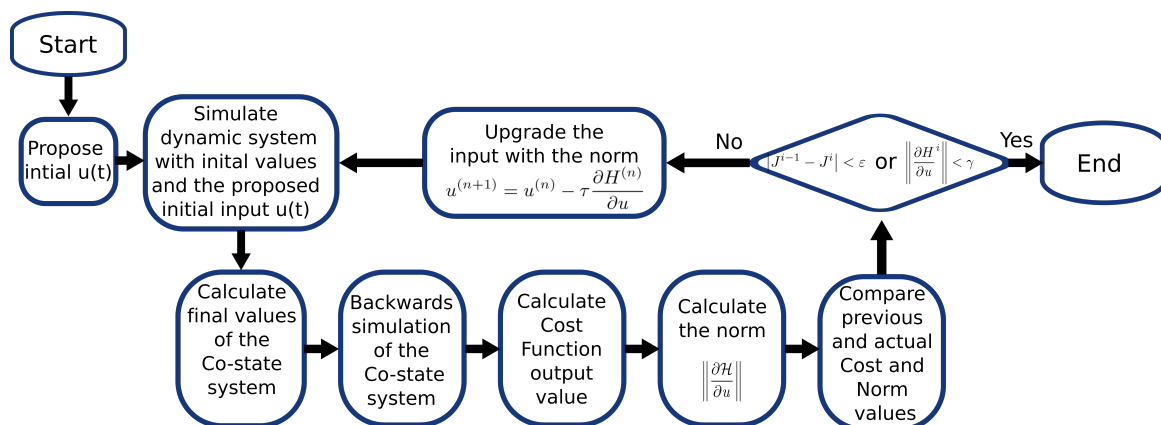


Figure 2. Flow diagram of the steepest descent method.

3.2. Finding Variable References

The optimization procedure seeks to find references for the velocity and flux; hence, it is convenient to define

$$u = \begin{bmatrix} u_\omega & u_\psi \end{bmatrix}^T = \begin{bmatrix} \omega_{ref} & \psi_{ref} \end{bmatrix}^T. \tag{24}$$

The main objective of this work is the reduction of energy consumption. Consequently, it is convenient to propose a function cost that depends on motor stator currents because these currents are directly related to the motor energy consumption.

Thus, the cost function is proposed as

$$J(u) = g_\omega (\omega_{ref} - \omega_r(t_f))^2 + \int_{t_0}^{t_f} \left((i_{ds}^s)^2 + (i_{qs}^s)^2 \right) dt. \tag{25}$$

Note that a big value of g_ω reinforces the fact that the final value of the velocity has been reached.

The overall system model is composed of the motor model and the controller model. Hence, the complete system dynamical equation is formed by the five differential equations of the motor given by Equation (1), the two flux estimator differential equations given by Equation (3), and the three differential equations of the PI controllers given by Equations (8)–(10). It is convenient to define the motor state using

$$x_m = \begin{bmatrix} i_{ds}^s & i_{qs}^s & \psi_{dr}^s & \psi_{qr}^s & \omega_r \end{bmatrix}^T. \tag{26}$$

The estimator state is defined by

$$x_e = \begin{bmatrix} \hat{\psi}_{dr}^s & \hat{\psi}_{qr}^s \end{bmatrix}^T \tag{27}$$

and the controllers state is defined by

$$x_c = \begin{bmatrix} \omega_{ie} & i_{ie} & \psi_{ie} \end{bmatrix}^T. \tag{28}$$

Hence, the complete system state can be defined by

$$x = \begin{bmatrix} x_m & x_e & x_c \end{bmatrix}^T. \tag{29}$$

According to Section 3.1, from Equations (25)–(28), the Hamiltonian can be expressed by

$$\mathcal{H}(x, u, p) = (i_{ds}^s)^2 + (i_{qs}^s)^2 + p(x, u)^T \dot{x}. \tag{30}$$

The co-state dynamical equations are obtained using

$$\dot{p} = -\frac{\partial \mathcal{H}}{\partial x}. \tag{31}$$

It is important to point out that, in addition to dynamical equation, the system description includes algebraic equations such as the Park and Inverse Park transformations (see Figure 1). Although, theoretically, these algebraic equations could be considered as additional restrictions, it is not convenient to do so. Including algebraic equations as restrictions means that the numerical algorithm has to solve them at each iteration. This significantly increases the time required for algorithm execution, and means that it is prone to errors and could result in numerical instability.

Instead of including algebraic relations as restrictions, they were solved and included in the system dynamical equations. Such dynamical equations were used in Equations (30) and to find the co-state equations from Equation (31). Note that the inclusion of algebraic equations in dynamical equations gives rise to very long expressions that are not written here because they do not add

clarity. However, they are not difficult to obtain using symbolic computation software, like Wolfram Mathematica (WM) (version 10.0.0.0, Wolfram Research Inc., Champaign, IL, USA).

According to Equation (20), the boundary values of co-states are zero, except for

$$p_{\omega}(t_f) = \omega_{ref} - \omega_r(t_f). \quad (32)$$

After determining all system and co-state dynamical equations and their boundary conditions, the steepest descent was applied to find the optimal functions for u . The initial time was zero and the final time t_f was proposed from a simulation without optimization. The norm employed was

$$\int_{t_0}^{t_f} \left[\left(\frac{\partial \mathcal{H}}{\partial u_{\omega}} \right)^2 + \left(\frac{\partial \mathcal{H}}{\partial u_{\psi}} \right)^2 \right] dt. \quad (33)$$

4. Simulation Results

Using WM, the ten differential equations of the complete system were obtained in explicit form. The developed code used the motor model, the flux estimator, and the controller equations. The ability of WM to manipulate symbolic expressions allows different dynamic systems with different parameters to be obtained with almost no effort. To actually obtain the references, optimization and simulation procedures were developed in Java. Methods to evaluate the cost functions and norm functions were also programmed. A translator between expressions produced by WM and expressions with the syntax of Java was also developed. The optimization algorithm was programmed in Java because calculations take less time to perform on this platform than in WM, and has more tools for debugging. Hence, it is easier to find and solve potential problems. Once the optimized references were obtained in Java, these functions were fed back to the motor model in WM. With this strategy, we ensured that well performing optimization and simulation procedures were developed.

The motor parameters used in the simulations are shown in Table 2. Such parameters were obtained from the 3/4 HP induction motor. The optimization parameters were $\tau = 0.01$ and $\max(\partial \mathcal{H} / \partial u) = 5(10^{-6})$.

Table 2. Motor parameters used in simulations.

Parameter	Value
Power	559.27 W
P	2
R_r	21.34 Ω
R_s	4.19 Ω
L_m	1.37 H
L_{ls}	0.05 H
L_{lr}	0.05 H
T_L	1.0 Nm
J	5.89×10^{-4} kg·m ²

Several simulations were performed to observe the behaviors of the supply currents and the angular velocity. The final angular velocity was restricted to keep voltage supply below 220VAC. In all simulation conditions, the current consumption and peak value reduction were observed. The percentage of energy consumption reduction was between 20 and 45% depending on the angular velocity and mechanical load.

In Figures 3 and 4, two of these simulations are shown. As can be observed from these simulations, the optimization procedure changed the references. As a consequence of this change, peak values were notably reduced. Particularly, it can be observed from the graphs that optimization of references $u_{\omega}(t)$ and $u_{\psi}(t)$ reduced the mechanic stress by reducing the peak angular velocity value and smoothing the acceleration. Optimization also reduced the peak values of i_{ds}^s and i_{qs}^s , which are the optimization

target variables. If the motor demands less current, the required voltage will be less. Reductions in the current and voltage peak values mean less peak power is needed.

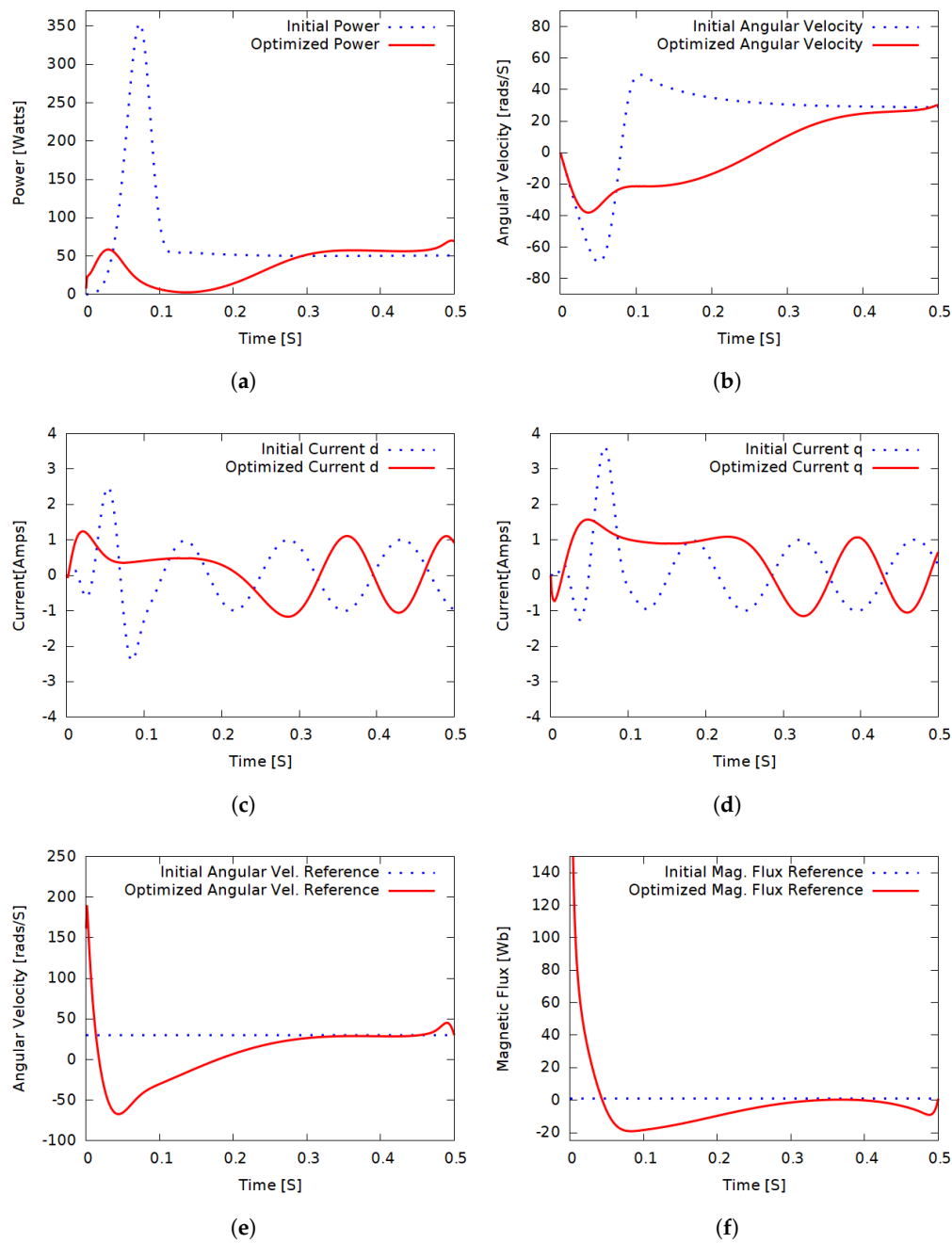


Figure 3. Simulation with load. Final velocity: 30 rads/s. Final time: 0.5 s. (a) motor power; (b) motor angular velocity; (c) motor supply current *d*-axis; (d) motor supply current *q*-axis; (e) angular velocity reference; (f) magnetic flux reference.

The level of reduction achieved is summarized in Tables 3 and 4. To obtain the values reported in these tables, the current consumption was calculated using

$$\int_{t_0}^{t_f} \left((i_{ds}^s)^2 + (i_{qs}^s)^2 \right) dt \tag{34}$$

and the energy consumed was calculated by

$$\frac{3}{2} \int_{t_0}^{t_f} (i_{ds}^s V_{ds}^s + i_{qs}^s V_{qs}^s) dt. \tag{35}$$

The average apparent power delivered by the power source was calculated from

$$AP_{Av} = \frac{3}{2} \sqrt{V_d^2 + V_q^2} \sqrt{i_d^2 + i_q^2}, \tag{36}$$

where V_d , V_q , i_d and i_q are the root mean square (RMS) values [24].

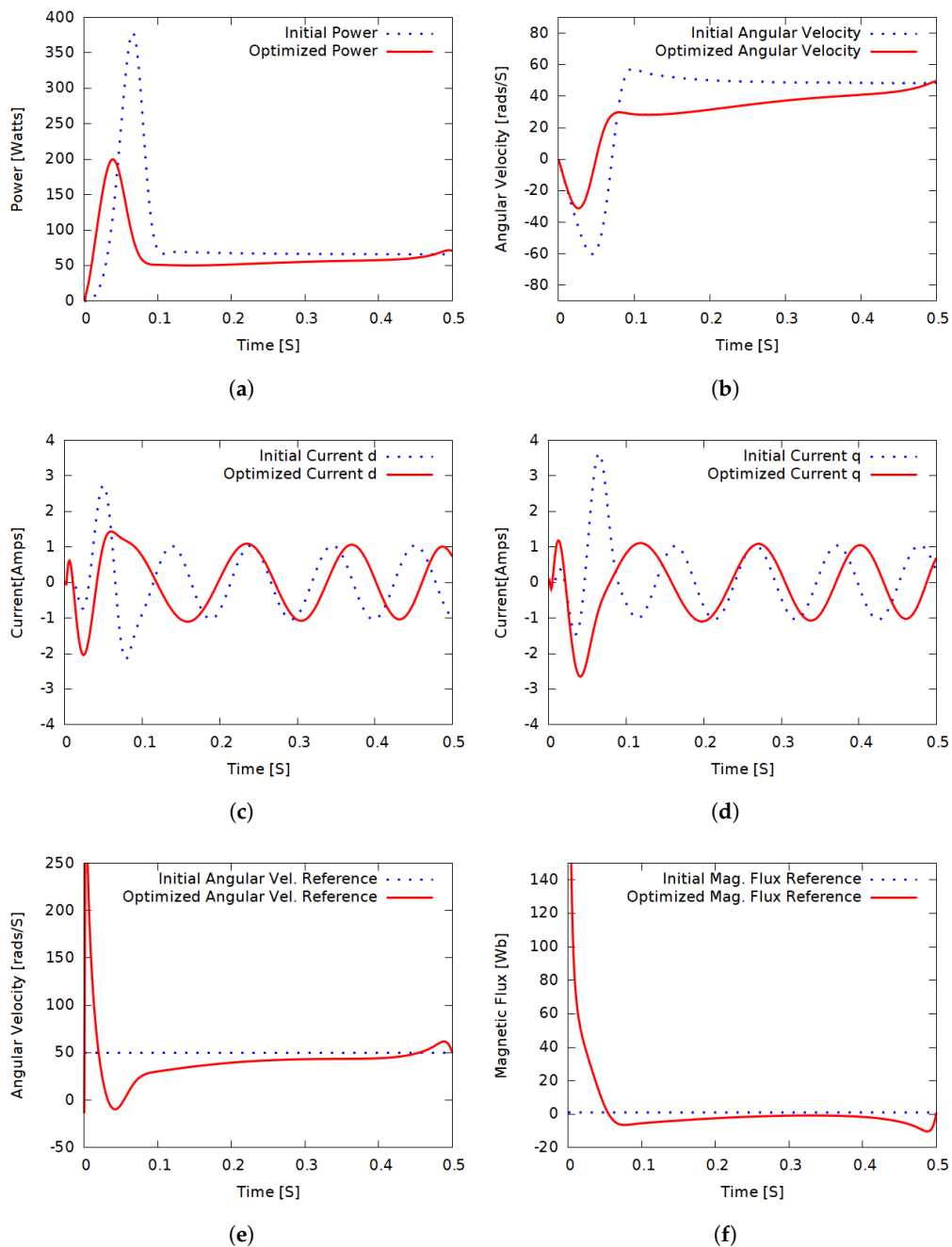


Figure 4. Simulation with load. Final velocity 50 rads/s. Final time: 0.5 s. (a) motor power; (b) motor angular velocity; (c) motor supply current d -axis; (d) motor supply current q -axis; (e) angular velocity reference; (f) magnetic flux reference.

Table 3. Simulation with load. Final velocity: 30 rads/s. Final time: 0.5 s.

Parameter	Original	Optimized	%
Peak Current	3.62 A	1.56 A	−56.9%
Peak Power	352.35 W	70.18 W	−80.08%
Energy	34.83 J	18.50 J	−46.88%
Apparent Average Power	103.73 VA	51.59 VA	−50.26%
Current Consumption	1.32 A ² ·s	1.13 A ² ·s	−14.4%

Table 4. Simulation with load. Final velocity: 50 rads/s. Final time: 0.5 s.

Parameter	Original	Optimized	%
Peak Current	3.54 A	2.62 A	−25.9%
Peak Power	378.01 W	199.73 W	−47.16%
Energy	42.52 J	32.58 J	−23.38%
Apparent Average Power	143.76 VA	110.01 VA	−23.47%
Current Consumption	1.34 A ² ·s	1.24 A ² ·s	−7.46%

Note that, instead of using the commonly used acceleration ramp, the proposed algorithm seeks the optimization of current consumption by applying large initial values at the set points and then rapidly converging them to the final value, which is equal to the original set-point value. The large initial set-point values help the system to have a faster response, but this faster response does not imply big peak values.

5. Conclusions

It has been shown in this work that, if a Field-Oriented Controlled induction motor has variable references for angular velocity and rotor magnetic flux, it can reduce the energy consumed by 20–45% and decrease the current consumption by 10–15%. A procedure to find these references was proposed. Variable current and flux references also reduce peak current values. This effect can reduce the stress over the electric installation; furthermore, acceleration peaks are lower than in the initial simulation reducing the mechanic stress of the motor and the load.

Due to its massive number of calculations, the proposed procedure to find variable references cannot be done during motor operation. If there is a change in parameters or mechanical load, the calculations must be redone. A plausible strategy is to perform the calculations for several common cases and use interpolation if another case arises during the operation. Nevertheless, there are significant motor applications where changes in velocity are known and the motor starts and stops continuously.

Author Contributions: Author contribution: conceptualization, J.R. and D.C.; methodology, J.R. and D.C.; software, J.R. and D.N.; validation, J.R. and D.N.; formal analysis, J.R. and D.C.; investigation, J.R. and D.C.; resources, D.C.; data curation, F.M.; writing—original draft preparation, J.R.; writing—review and editing, F.M. and D.N.; visualization, J.R.; supervision, D.C. and F.M.; project administration, D.C.; funding acquisition, D.C.

Funding: This research was funded by Instituto Politecnico Nacional under grant number SIP-20181542.

Conflicts of Interest: The authors declare no conflict of interest.

References

1. Waide, P.; Brunner, C.U. *Energy-Efficiency Policy Opportunities for Electric Motor-Driven Systems*; IEA Energy Papers 2011/7; OECD Publishing: Paris, France, 2011.
2. Ferreira, F.J.T.E.; de Almeida, A.T. Overview on energy saving opportunities in electric motor driven systems—Part 1: System efficiency improvement. In Proceedings of the 2016 IEEE/IAS 52nd Industrial and Commercial Power Systems Technical Conference (I CPS), Detroit, MI, USA, 1–5 May 2016; pp. 1–8. [[CrossRef](#)]

3. Stumper, J.; Kennel, R. Real-time dynamic efficiency optimization for induction machines. In Proceedings of the 2013 American Control Conference, Washington, DC, USA, 17–19 June 2013; pp. 6589–6594. [CrossRef]
4. Bazzi, A.M.; Krein, P.T. Review of Methods for Real-Time Loss Minimization in Induction Machines. *IEEE Trans. Ind. Appl.* **2010**, *46*, 2319–2328. [CrossRef]
5. Ghozzi, S.; Jelassi, K.; Roboam, X. Energy optimization of induction motor drives. In Proceedings of the 2004 IEEE International Conference on Industrial Technology, 2004, Hammamet, Tunisia, 8–10 December 2004; Volume 2, pp. 602–610. [CrossRef]
6. Thangaraj, R.; Chelliah, T.R.; Pant, M.; Abraham, A.; Grosan, C. Optimal gain tuning of PI speed controller in induction motor drives using particle swarm optimization. *Log. J. IGPL* **2011**, *19*, 343–356. [CrossRef]
7. Mitsukura, Y.; Yamamoto, T.; Kaneda, M. A design of self-tuning PID controllers using a genetic algorithm. In Proceedings of the 1999 American Control Conference (Cat. No. 99CH36251), San Diego, CA, USA, 2–4 June 1999; Volume 2, pp. 1361–1365. [CrossRef]
8. Mohamed, H.A.F.; Lau, E.L.; Yang, S.S.; Moghavvemi, M. Fuzzy-SMC-PI Flux and Speed Control for Induction Motors. In Proceedings of the 2008 IEEE Conference on Robotics, Automation and Mechatronics, Chengdu, China, 21–24 September 2008; pp. 325–330. [CrossRef]
9. Taheri, A.; Rahmati, A.; Kaboli, S. Efficiency Improvement in DTC of Six-Phase Induction Machine by Adaptive Gradient Descent of Flux. *IEEE Trans. Power Electron.* **2012**, *27*, 1552–1562. [CrossRef]
10. Hung, N.T.; Thien, N.C.; Nguyen, T.P.; Le, V.S.; Tuan, D.A. *Optimization of Electric Energy in Three-Phase Induction Motor by Balancing of Torque and Flux Dependent Losses*; AETA 2013: Recent Advances in Electrical Engineering and Related Sciences; Zelinka, I., Duy, V.H., Cha, J., Eds.; Springer: Berlin/Heidelberg, Germany, 2014; pp. 497–507.
11. Melo, P.; de Castro, R.; Araujo, R.E. Evaluation of an Energy Loss-Minimization Algorithm for EVs Based on Induction Motor. In *Induction Motors*; IntechOpen: Rijeka, Croatia, 2012; Chapter 17, doi:10.5772/52280.
12. Thanh Hung, N.; Chi Thien, N.; Phuong Nguyen, T.; Thus, Le, V.; Anh Tuan, D. Optimization of Electric Energy in Three-Phase Induction Motor by Balancing of Torque and Flux Dependent Losses. *Lect. Notes Electr. Eng.* **2014**, *282*, 497–507. [CrossRef]
13. Borisevich, A. Numerical Method for Power Losses Minimization of Vector-Controlled Induction Motor. *Int. J. Power Electron. Drive Syst.* **2015**, *6*, 486–497. [CrossRef]
14. Ta, C.M.; Hori, Y. Convergence improvement of efficiency-optimization control of induction motor drives. *IEEE Trans. Ind. Appl.* **2001**, *37*, 1746–1753. [CrossRef]
15. Ismail, M. Efficiency optimisation with PI gain adaptation of field-oriented control applied on five phase induction motor using AI technique. *Int. J. Model.* **2013**, *20*, 344–360. [CrossRef]
16. Wilson, D. Teaching Your PI Controller to Behave. 2015. Available online: <http://www.webcitation.org/78mq5YtqU> (accessed on 31 May 2019).
17. Bose, B. *Modern Power Electronics and AC Drives*; Prentice Hall: Upper Saddle River, NJ, USA, 2001.
18. Krishnan, R. *Electric Motor Drives: Modeling Analysis In addition, Control*; Prentice-Hall Of India Pvt. Limited: New Delhi, India, 2008.
19. De Doncker, R.; Pulle, D.; Veltman, A. *Advanced Electrical Drives: Analysis, Modeling, Control*; Power Systems; Springer: Berlin/Heidelberg, Germany, 2010.
20. Duesterhoeft, W.C.; Schulz, M.W.; Clarke, E. Determination of Instantaneous Currents and Voltages by Means of Alpha, Beta, and Zero Components. *Trans. Am. Inst. Electr. Eng.* **1951**, *70*, 1248–1255. [CrossRef]
21. Kirk, D. *Optimal Control Theory: An Introduction*; Dover Books on Electrical Engineering; Dover Publications: Englewood Cliffs, NJ, USA, 2004.
22. Cassel, K. *Variational Methods with Applications in Science and Engineering*; Cambridge University Press: New York, NY, USA, 2013.
23. Liberzon, D. *Calculus of Variations and Optimal Control Theory: A Concise Introduction*; Princeton University Press: Princeton, NJ, USA, 2012.
24. Reginatto, R.; Ramos, R.A. On electrical power evaluation in dq coordinates under sinusoidal unbalanced conditions. *IET Gener. Transm. Distrib.* **2014**, *8*, 976–982. [CrossRef]

